

Author contribution section

LB: Conceptualization, Investigation, Methodology, Formal Analysis, Data curation, Writing- Original draft, Visualization, Writing - Reviewing and Editing,

AG: Investigation, Data curation, Writing- Original draft preparation.

CC: Project administration, Resources, Supervision, Writing- Original draft.

LR: Conceptualization, Methodology, Formal Analysis, Supervision, Writing- Original draft preparation, Visualization, Writing - Reviewing and Editing.

Journal Pre-proof

Parietal tACS at beta frequency improves vision in a crowding regime

Luca Battaglini^{1,2}, Andrea Ghiani¹, Clara Casco^{1,2} & Luca Ronconi^{3,4}

¹ Department of General Psychology, University of Padova (Italy)

² Neuro.Vis.U.S. Laboratory, University of Padova, Padova, Italy

³ Faculty of Psychology, Vita-Salute San Raffaele University, Milan, Italy

⁴ Division of Neuroscience, IRCCS San Raffaele Scientific Institute, Milan, Italy

Corresponding author:

Luca Ronconi, PhD

Faculty of Psychology, Vita-Salute San Raffaele University

Via Olgettina 58, 20132, Milan (Italy).

Email: ronconi.luca@univr.it

Phone: +390226434887

Running title: *Parietal tACS reduces visual crowding*

Disclosure of potential conflict of interest: The authors declare no competing interests.

20 **ABSTRACT**

21 Visual crowding is the inability to discriminate objects when presented with nearby flankers and
22 sets a fundamental limit for conscious perception. Beta oscillations in the parietal cortex were found
23 to be associated to crowding, with higher beta amplitude related to better crowding resilience. An
24 open question is whether beta activity directly and selectively modulates crowding. We employed
25 transcranial alternating current stimulation (tACS) in the beta band (18-Hz), in the alpha band (10-
26 Hz) or in a sham regime, asking whether 18-Hz tACS would selectively improve the perception of
27 crowded stimuli by increasing parietal beta activity. Resting electroencephalography (EEG) was
28 measured before and after stimulation to test the influence of tACS on endogenous oscillations.
29 Consistently with our predictions, we found that 18-Hz tACS, as compared to 10-Hz tACS and
30 sham stimulation, reduced crowding. This improvement was found specifically in the contralateral
31 visual hemifield and was accompanied by an increased amplitude of EEG beta oscillations,
32 confirming an effect on endogenous brain rhythms. These results support a causal relationship
33 between parietal beta oscillations and visual crowding and provide new insights into the precise
34 oscillatory mechanisms involved in human vision.

35

36

37 **Keywords:** neurostimulation, perception, vision, tACS, tES

38 INTRODUCTION

39 Visual crowding is one of the factors that most impairs visual object recognition and for this reason,
40 it can be considered as a fundamental bottleneck for conscious object perception (Levi, 2008).

41 Crowding can be defined as the deleterious influence of nearby contours on visual discrimination. It
42 is a perceptual phenomenon typical of peripheral vision that limits recognition and it can be
43 observed with simple objects, such as oriented gratings, and also with complex objects, such as
44 letters and faces (Levi, 2008; Pelli, 2008; Whitney and Levi, 2011). For example, crowding limits
45 the perception of elementary contours in the periphery (May and Hess, 2007), the pre-processing of
46 the parafoveal word letters (Moll and Jones, 2013) and limits also the ability to recognize peripheral
47 target in a field of distracting object in demanding tasks such as action videogames (Green and
48 Bavelier, 2007).

49 Psychophysical studies have greatly contributed to the understating of visual crowding (for reviews
50 see (Herzog and Manassi, 2015; Levi, 2008; Pelli, 2008) by showing, for example, that the main
51 factor that modulates visual crowding is the distance between target and flankers. Moreover, among
52 the main properties of crowding we have eccentricity dependence, size independence, inward-
53 outward anisotropy and radial/tangential anisotropy (Levi, 2008).

54 Despite the large amount of psychophysical studies on crowding, its neural substrates are still
55 unclear. A better understanding of the neural bases of crowding may help clarifying the
56 mechanisms responsible of crowding and could give important insights for developing
57 neurorehabilitation trainings. In particular, the improvement of perception in a crowding regime is a
58 rehabilitation goal in clinical populations that are associated to excessive crowding, such as
59 developmental dyslexia and amblyopia (Bertoni et al., 2019; Bonneh et al., 2007; Gori and Facoetti,
60 2015; Zorzi et al., 2012).

61 Visual crowding is considered as a heterogeneous phenomenon generally occurring because the
62 output of detectors activated by several simple features belonging to the target is inappropriately
63 integrated to the output of detectors responding to non-target features (Chakravarthi and Pelli,

2011). There is general consensus that the more complex the object, the higher the visual area responsible for crowding: excessive integration may occur at an early level of visual processing where binding of elementary contour features occurs (Freeman and Simoncelli, 2010; Pelli, 2008) or at a higher level, for example in ventral area V4, that mediates integration of object contours. Moreover, bottom-up processing in the dorsal stream also contributes to crowding. Contour integration in normal vision is facilitated by coarse representation of visual input achieved by bottom-up dorsal processing. Through recursive feedback from the parietal cortex, the major projection of the dorsal stream, this low-frequency representation drives binding mechanisms towards the stimulus configuration and facilitates attention-demanding identification tasks in the ventral stream (Levy et al., 2010; Vidyasagar, 2004, 1999). In principle, the same re-entrant information from the dorsal stream would promote binding between target and flankers in a crowded regime and would limit segmentation of the target from flankers in the peripheral field (Chakravarthi and Pelli, 2011; Omtzigt et al., 2002). However, when the task needs an uncrowded perceptual solution, the dorsal-to-ventral feedback mediates segmentation of the target letter from the flankers through activation of receptive fields of appropriate size (Lamme and Roelfsema, 2000; Lee et al., 1998).

A promising approach to enlighten the mechanisms of crowding is that of the studies employing electroencephalography (EEG). Recently, EEG studies were performed by using complex stimuli configurations (e.g. Vernier stimuli, letters) found that crowding induced a lower amplitude of a late visual event-related potential (ERP) component (i.e., the N1), peaking around 200/250 ms post-stimulus (Chicherov et al., 2014; Ronconi et al., 2016). Chen and colleagues (Chen et al., 2014), used simple gratings as target stimuli and showed that the C1 component in the ERPs, reflecting activity in early visual areas (Di Russo et al., 2002), was suppressed in a crowded condition, but also significantly modulated by attention. In a more recent study, Han and Luo (Han and Luo, 2019) employed EEG in combination with a temporal response function (TRF) approach. They showed the presence of two components in the target-specific TRF response: an early component in

90 occipital channels and a late component (starting from ~200 ms) in fronto-parietal channels. This
91 late fronto-parietal component correlated, as opposed to the occipital component, with target
92 discrimination in the crowded condition. Overall, the picture emerging from these recent studies
93 shows that visual crowding emerges in the EEG (Han and Luo, 2019) and ERPs (Chicherov et al.,
94 2014; Ronconi et al., 2016) (i.e. N1) with timing and scalp distribution that are typically associated
95 with later stages of stimulus processing, or alternatively appears at earlier stages but are influenced
96 by dorsal/attentional feedback modulation (Chen et al., 2014; Peng et al., 2018).

97 Another fundamental approach to understand the neural mechanisms of crowding is the analysis of
98 its oscillatory correlates. In two recent studies, Ronconi and colleagues (Ronconi et al., 2016;
99 Ronconi and Bellacosa Marotti, 2017) found a relationship between visual crowding and EEG
100 oscillations in the beta band (15-30 Hz). In particular, Ronconi et al. (Ronconi et al., 2016)
101 measured crowding in different conditions of spacing between target and flankers and found a
102 stronger post-stimulus beta power reduction in the strong crowding condition (smaller target-
103 flankers distance) relative to the weak crowding condition. Moreover, stronger beta power reduction
104 correlated to individual task performance that was more disturbed by visual crowding. Ronconi and
105 Bellacosa Marotti (2017) further confirmed the relationship between beta band oscillations and
106 visual crowding, by showing that beta power before the time of the stimulus onset was higher in
107 frontal and parieto-occipital sensors for trials where participants correctly discriminated the target
108 letter among flankers, but only in the strong, not in the weak, crowding condition.

109 Although there is evidence of a strong relationship between ongoing neural oscillations and
110 crowding phenomenon, a causal relationship can only be found by means of a direct modulation of
111 these neural oscillations. In particular, tACS seems a particularly appropriated method to directly
112 modulate oscillatory signals. Some studies indeed showed that tACS is able to interact with the
113 brain's natural cortical oscillations causing entrainment (Fröhlich and McCormick, 2010; Helfrich
114 et al., 2014) and driving the activity of cortical regions to the frequency imposed by tACS.
115 Moreover, tACS dependent behavioural effects on sensory and cognitive processes have been

116 shown (Herrmann et al., 2016). In vision for example, Laczo and colleagues (Laczó et al., 2012)
117 showed that tACS at 60 Hz over the visual cortex increased contrast perception compared to tACS
118 at 40 and 80 Hz. In addition, tACS in the gamma frequency has been shown to modulate perception
119 of bistable motion (Strüber et al., 2014). Moreover, tACS at theta frequency over the right parietal
120 cortex increased visual working memory (Bender et al., 2019; Wolinski et al., 2018).

121 The present study was based on the evidence reviewed above of a relationship between visual
122 crowding and EEG oscillations in the beta band (15-30 Hz) and on the evidence that tACS can be
123 used as a method to modulate perceptually relevant brain oscillations. With these premises, tACS
124 seems appropriate to assess a direct role of beta frequency range (13-20 Hz) in reducing crowding.

125 tACS was delivered on the right parietal cortex for different reasons. First, previous EEG studies
126 showed that the strongest beta modulation was evident in a cluster of right occipito-parietal
127 channels (Ronconi et al., 2016; Ronconi and Bellacosa Marotti, 2017). Second, the N1 component
128 of the ERPs, which is the main component reflecting crowding as introduced above (Chicherov et
129 al., 2014; Ronconi et al., 2016), originates mainly from cortical sources in the right parietal cortex,
130 as found in previous visual perception studies that did (Chicherov et al., 2014) or did not (Di Russo
131 et al., 2002) directly manipulate the crowding strength. Third, Romei and colleagues (Romei et al.,
132 2012, 2011) used rhythmic TMS over the right and left parietal cortex to entrain oscillatory activity
133 in the theta, beta and alpha band aimed at modulating local and global attention in a Navon task.

134 The authors found that beta stimulation of the right (but not left) parietal cortex (Romei et al., 2011)
135 facilitated local processing. In addition, beta band EEG activity is selectively predictive of parietal
136 cortex excitability when probing TMS-induced phosphene perception (Cabral-Calderin and Wilke,
137 2019; Samaha et al., 2017). We also reasoned that beta modulation of parietal cortex with
138 consequences on crowding would ultimately confirm a role of dorso-ventral feedback in such task
139 (Lamme and Roelfsema, 2000; Robol et al., 2013). The role of beta tACS (18 Hz) in reducing
140 crowding was compared to that of two control stimulations on the same cortical site: i) a sham (no
141 stimulation) and ii) a 10-Hz tACS (i.e. within alpha band, which has not been shown to affect

142 crowding (Ronconi et al., 2016; Ronconi and Bellacosa Marotti, 2017). To test the hypothesis that
 143 tACS can lead to changes of endogenous brain rhythm (Fröhlich and McCormick, 2010; Helfrich et
 144 al., 2014), we recorded the resting-state EEG signal, to test pre- and post-stimulation power
 145 differences in the relevant frequency bands (beta and alpha).

146

147 **METHOD**

148 *Participants*

149 Twenty participants (10 male, mean age = 23.05, age range = 18 – 33) took part in this study. They
 150 were all students from the University of Padova. They provided informed consent, had normal or
 151 corrected to normal vision and normal hearing. All of them met the criteria for the application of
 152 Transcranial Alternating Current Stimulation (tACS) (Antal et al., 2017). This experiment has been
 153 approved by the Ethics Committee of the Department of General Psychology at the University of
 154 Padua (protocol n. 2598).

155

156 *Stimuli*

157 Participants performed the task in a dimly lit room and viewed stimuli binocularly on a 19” LCD
 158 Asus monitor with 60 Hz refresh rate. Stimuli were displayed on a mid-level gray background with
 159 40 cd/m² luminance. They were created via Psychtoolbox for Matlab (Brainard, 1997; Pelli, 1997)
 160 and consisted of 1.5 x 1.5 deg gaborized H-like and T-like configurations. Gabors that formed each
 161 stimulus were obtained through a product of an oriented sinewave grating and a circular Gaussian
 162 window according to the following formula:

$$G(x, y) = e^{-\frac{(x^2+y^2)}{2\sigma^2}} \times \cos\left[\frac{2\pi \times (\cos(\theta x) + \sin(\theta y))}{s + p}\right]$$

163

164 In this equation, the orientation θ could be either 0 deg for vertical and 90 deg for horizontal
 165 gabors. The phase of the sinusoid (p) was set on 90 deg. The spatial frequency (s) of the elements

166 was 2 c/deg and the standard deviation of the Gaussian window (σ) was .12 deg. Stimuli were
167 presented at full contrast (Michelson). On each trial, stimuli were built as follows. We designed a
168 matrix of the size of the stimulus. We divided it into a 5 x 5 grid of equally spaced x,y locations.
169 The gabors were then placed along the path of the letter (H or T). We used 9 patches for the Ts and
170 13 for the Hs. Centre-to-centre distance between adjacent patches was constant at .3 deg. Patches
171 could be both horizontal and vertical.

172

173 ***Procedure***

174 We implemented an orientation discrimination task with MATLAB Psychtoolbox (Brainard, 1997;
175 Pelli, 1997). The task was structured as follows: a fixation point was displayed for 2 seconds, then
176 the target T was randomly presented for ~50 ms to the left or to the right of the fixation point at 11
177 degrees of eccentricity (this duration is not enough to execute a saccade towards the stimulus). Ts
178 could have 4 possible orientations (0-270 deg in step of 90 deg) and they were vertically flanked by
179 H letters which could have 7 possible distances from the target (1 = 1.90 deg; 2 = 2.27 deg; 3 = 2.65
180 deg; 4 = 3.02 deg; 5 = 3.40 deg; 6 = 3.78 deg; 7 = 4.15 deg). A blank screen was shown for 2
181 seconds and finally a response display showed the 4 possible T rotations and the corresponding
182 response keys. One second after response, a new trial started. Participants were asked to recognize
183 the rotation of the Ts presented in each trial, keeping their fixation on the central point displayed for
184 the entire trial duration.

185 Each subject repeated the task three times with three different stimulation conditions, which were
186 randomized across participants: 10 Hz, 18 Hz and sham. 10 Hz was chosen as the frequency laying
187 at the center of the alpha band (8-12 Hz). 18 Hz was chosen because it was the frequency reflecting
188 the greatest amplitude modulation (i.e. power decrement) previous EEG study (Ronconi et al.,
189 2016). In the Supplementary Figure 1, we plotted EEG power of channel P4 in the beta range
190 extracted from our previous study in support of our choice of using this precise stimulation
191 frequency.

192 Each session lasted 45 minutes. The three sessions took place always in three different days. Each
193 session provided two small breaks after 15 and 30 minutes in order to prevent fatigue (tACS,
194 however, was on during the entire session). On average participants completed 512 trials in the
195 sham condition (SD=44; mean left hemifield trials =251; mean right hemifield trials =261), 508
196 trials in the 10-Hz session (SD=49; mean left hemifield trials =250; mean right hemifield trials
197 =258) and 513 trials in the 18-Hz session (SD=53; mean left hemifield trials =254; mean right
198 hemifield trials =259). All participants were unaware of the specific tACS protocol that was
199 administered on each session, thus resulting in a single blind procedure.

200

201 ***Stimulation setting and EEG recording***

202 tACS was applied through a StarStim8 device, a hybrid wireless neurostimulation system for
203 concurrent EEG/tACS controlled by the software Neuroelectronics Instrument Controller (*NIC 2.0*;
204 <http://www.neuroelectronics.com/products/software/nic2/>). The system had 8 channels that could be
205 located in 39 possible scalp positions through a neoprene headcap and according to the 10-10
206 system. We used 5 PISTIM Ag/AgCl electrodes with 1 cm radius both for stimulation and EEG
207 recording and 3 GELTRODE Ag/AgCl electrodes just for EEG recording. The stimulation setting
208 was set as follows: the stimulation electrode was placed in P4, while the 4 return electrodes were
209 placed in C4, Pz, O2 and P8. Stimulation intensity was set at 0.8 mA (*milliAmpere*), with offset set
210 at 0 mA; this value chosen following the most recent guidelines for tACS safety guidelines
211 considering a session duration of 40 minutes (Antal et al., 2017). This montage was chosen after
212 carefully evaluating the electric field distribution with the software NIC 2.0. In particular, this high-
213 density montage centred on P4 was optimal to stimulate the right parietal cortex (see Figure 1). We
214 created three protocols with different stimulation frequencies: 10 Hz, 18 Hz and Sham. It is
215 important to note that none of the participants reported the presence of retinal phosphenes nor with
216 10-Hz neither with 18- Hz tACS. Moreover, only two participants reported mild skin sensation (see
217 questionnaire in Fertoni et al., 2015) that disappeared after a few seconds of stimulation. All the

218 other participants did not report skin sensation. All subjects were asked at the end of the experiment
219 whether they could guess the presence of stimulation and were at chance level (see Supplementary
220 Table 1). About the EEG setting, the signal was recorded at a sampling frequency of 500 Hz and
221 with a 24-bit digitization using 8 electrodes positioned on the following scalp locations: C4, Pz, P4,
222 P8, PO8, PO7, Oz, O2. Channels activity was online referenced to Cz and the impedance was kept
223 below 10k Ω . EEG signal was recorded during an eyes-closed resting-state period of 3 minutes
224 immediately before and immediately after tACS application.

225

226 *Data analysis: behavioural data*

227 We calculated the proportion of correct response as a function of the target-flankers distance. Data
228 were then fitted with a logistic function (maximum likelihood criterion) by using the routines
229 provided by the Palamedes toolbox (Prins and Kingdom, 2018). The psychometric function was
230 created according to the following formula:

$$P(C; \alpha, \beta, \gamma; \lambda) = \gamma + \frac{1 - \gamma - \lambda}{1 + e^{-\beta(C-\alpha)}}$$

231 The inferior asymptote γ was set to a probability of 0.25 corresponding to the chance level. The
232 superior asymptote λ was fixed by setting the lapse rate to 0.02. α and β parameters were left free.
233 α corresponds to the threshold, β corresponds to the function's slope. In this study, the threshold is
234 the target-flanker distance (deg) related to a probability of 0.625 to give a correct response. This
235 value lies between the probability of best performance (1=100% of correct response) and the chance
236 level (0.25).

237 To analyse the effect of tACS on crowding, we performed a repeated measures analysis of variance
238 (ANOVA) on both the slope and threshold values with two within subject factors: Stimulation
239 Condition (10 Hz vs 18 Hz vs Sham) and Target Position (left vs right).

240

241 *Data analysis: Resting state EEG data*

242 Offline, eyes closed resting EEG data were band-pass filtered between 0.05 and 40 Hz (Butterworth
243 filter, order=2). The continuous data were segmented into 1-sec epochs to obtain a total 180 epochs
244 for both pre- and post- tACS periods. These epochs were visually inspected to remove data
245 segments contaminated by muscular or ocular artefacts (mean \pm SD of retained epochs after
246 artefacts rejection were: 177.88 ± 3.54 across all conditions). An independent component analysis
247 (ICA), estimated together for the pre- and post- tACS sessions, was used to correct for electrodes
248 artifacts when needed, resulting in a single ICA component that was removed in 8 out of 60
249 experimental sessions. The cleaned epochs were then used to extract the FFT spectrum. Zero
250 padding was applied (N=2000 samples) to increase the frequency resolution and data were baseline
251 normalized (dB) to the average epoch power. Finally, the individual power values in the frequency
252 range of interests were averaged for each participant and separately for the pre- and post-stimulation
253 sessions.

254 Hereafter, we will refer to ‘alpha power’ to indicate the average of power values extracted in the
255 frequency range between 8 and 12 Hz. Similarly, we will refer to ‘beta power’ to indicate the
256 average of power values extracted in the frequency range between 15 and 25 Hz. Differences in
257 alpha and beta power before and after tACS were tested at the channel P4 with paired samples t-
258 tests. Bonferroni correction was applied to account for the multiple comparisons (i.e. number of
259 channels). Data analysis was performed using Matlab (MathWorks, Inc., Natick, MA) and
260 EEGLAB (Delorme and Makeig, 2004).

261

262 ***Data analysis: relationship between tACS phase and perception***

263 In order to study how the phase of the external stimulation influences crowding accuracy, we used
264 the tACS sinewave to extract with a Hilbert transform the phase points (in radian) for each temporal
265 point during the stimulation session. This allowed us to obtain a phase value corresponding to the
266 presentation of the target in each trial. We created then six bins, evenly sized and non-overlapping,
267 ranged as follows: $[-\pi; -2/3\pi]$, $[-2/3\pi; -1/3\pi]$, $[-1/3\pi; 0]$, $[0; 1/3\pi]$, $[1/3\pi; 2/3\pi]$, $[2/$

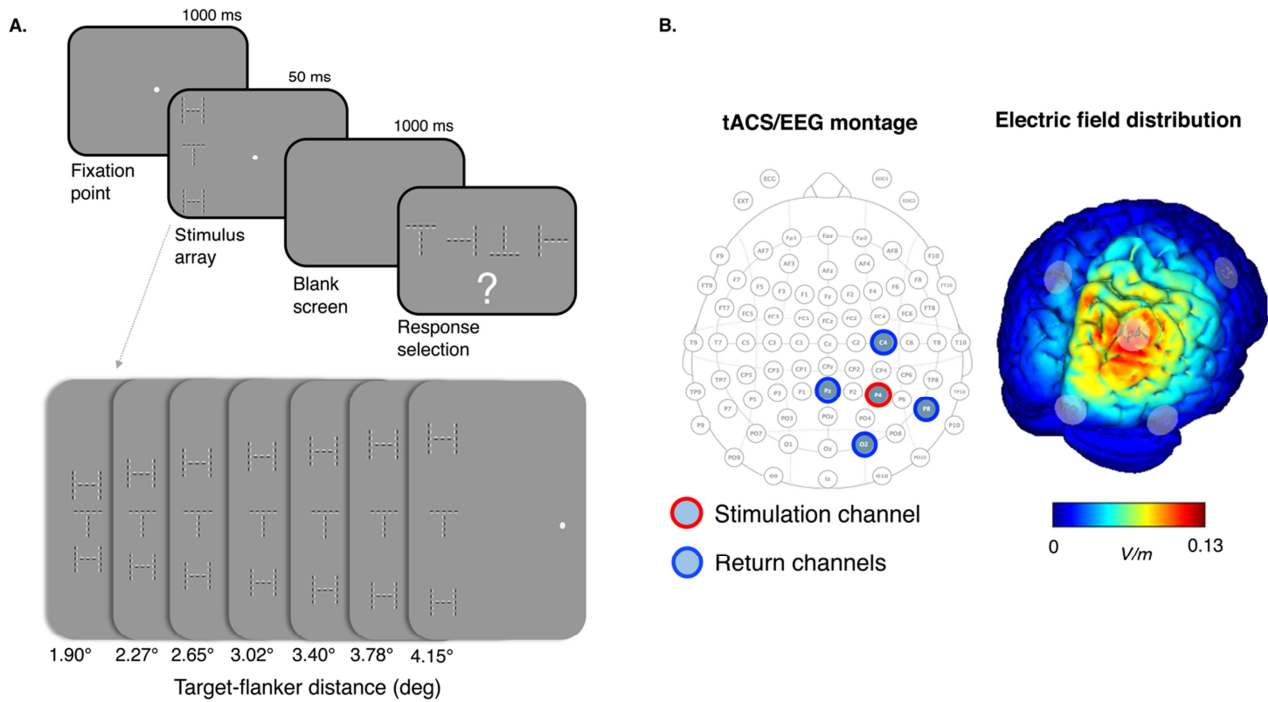
268 $3\pi; \pi]$ (in radians). Each bin contained on average 42.6 trials for the 18-Hz condition (SD=3.7) and
269 43.3 trials for the 10-Hz condition (SD=3.8).

270 The analysis above, however, does not evaluate whether the modulation of performance as a
271 function of tACS phase has a sinusoidal shape as predicted by a true neural entrainment effect.
272 Thus, we performed a second analysis where we first averaged the data across participants and then
273 we calculated the best fitting sinusoidal function separately for target hemifield (left vs. right) and
274 tACS frequency (10 vs. 18 Hz). The sinusoidal function used a fixed frequency (i.e. one cycle
275 across the datapoints) but free amplitude and phase, similarly to other previous studies (e.g. Stonkus
276 et al., 2016). The goodness of fit (R^2) of the resulting best fitting function for the observed data was
277 compared with a null distribution obtained with 1000 permutations of the real data. Specifically, for
278 each individual dataset we calculated 1000 permutations by randomizing the phase bin label.
279 Permuted data were averaged across participants and the 1000 measures of goodness of fit obtained
280 from these permuted data constituted the null distribution against which we could compare the
281 goodness of fit obtained from the real data and extract the p-value.

282

283

[Figure 1 about here]



284

285

286 Figure 1. (A) Illustration of a trial example and of the different target-flankers distances used in the crowding task. (B)

287 tACS/EEG montage and the electric field distribution on the cortical surface; as it can be seen, the maximum current

288 density was induced on the right parietal cortex.

289

290 RESULTS

291 *18-Hz tACS diminished the effect of crowding on perception*

292 The individual fitting of the psychometric function¹ provided the following goodness-of-fit

293 measures (pDev; Kingdom and Prins 2016) in terms of mean±SD: left hemifield target with sham

294 tACS=0.52±0.27, right hemifield target with sham tACS=0.59±0.24, left hemifield target with 10

295 Hz tACS=0.53±0.32, right hemifield target with 10 Hz tACS=0.52±0.35, left hemifield target with

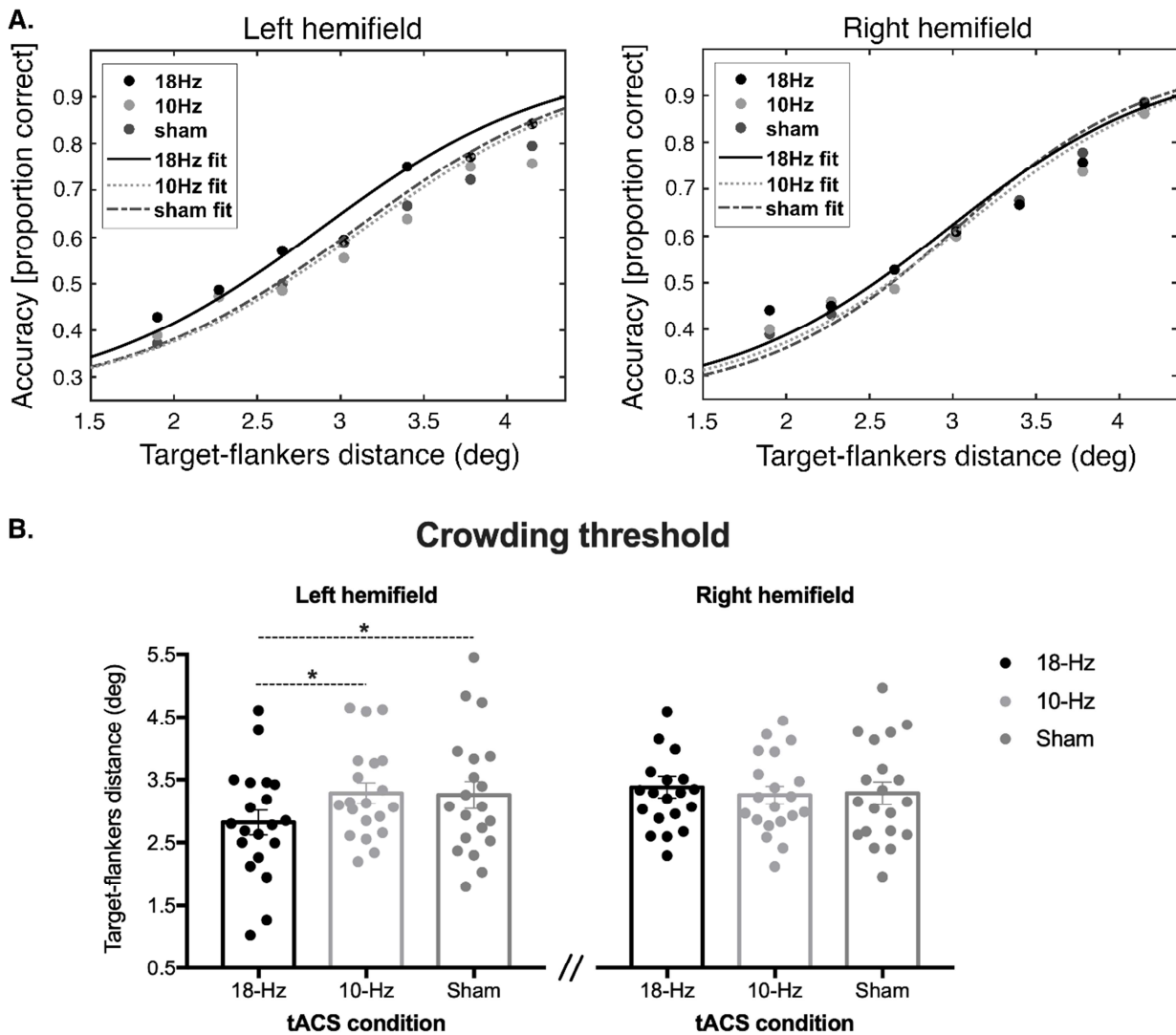
296 18 Hz tACS=0.47±0.29, right hemifield target with 18 Hz tACS=0.53±0.28.

¹ Raw data that were fitted with psychometric functions contained only 2 outliers out of 840 data points (> 3 standard deviations). Additional analysis taking into account outliers and further explanation about the Palamedes fitting routines can be found in the Supplementary Material).

297 Threshold values were submitted to a repeated measures ANOVA with two within subject factors:
298 Stimulation Condition (10 Hz vs 18 Hz vs Sham) and Target Position (left vs right). The ANOVA
299 did not show a significant main effect of the Stimulation Condition ($F_{(2,38)} = 1.71, p = .19; \eta^2_p = .08$)
300 and Target Position ($F_{(1,19)} = 1.32, p = .26; \eta^2_p = .06$). Importantly, a significant interaction
301 Stimulation Condition \times Target Position was found ($F_{(2,38)} = 6.70, p = .003; \eta^2_p = .26$). Post hoc
302 comparison (t-test Bonferroni corrected) revealed lower threshold value (shorter distance target-
303 flankers at 0.625 proportion of correct response) for stimuli presented in the left visual hemifield
304 (contralateral to the stimulation) during the tACS session at 18 Hz compared to 10 Hz ($t_{(19)} = 3.03;$
305 $p_{corr} = .02$; Cohen's $d=0.67$) and sham session ($t_{(19)} = 2.70; p_{corr} = .042$; Cohen's $d=0.6$) (Figure 2).
306 On the contrary, for stimuli presented in the right visual hemifield (ipsilateral to the stimulation) no
307 effects of tACS was evident (all $ps > .99$).

308 The ANOVA on slope values, on the contrary, did not reveal main effects of Stimulation Condition
309 ($F_{(1.28,24.4)} = 0.95, p = .39; \eta^2_p = .05$) or Target Position ($F_{(1,19)} = 3.56, p = .07; \eta^2_p = .16$), nor a
310 significant interaction ($F_{(1.22,23.19)} = 1.38, p = .36; \eta^2_p = .07$).

311 [Figure 2 about here]



312

313 Figure 2. Beta tACS improved crowded perception. (A) Psychometric functions obtained from the mean data with 18-
 314 Hz tACS (black line), 10-Hz (grey dotted line) and sham (dark grey broken line). Dots represent mean accuracy as a
 315 function of target-flanker distance (18-Hz tACS: black dots, 10-Hz tACS: grey dots, sham: dark grey dots). (B)
 316 threshold values obtained with 18-Hz, 10-Hz tACS and sham for the left and right hemifield. * indicates pvalue < 0.05
 317 (Bonferroni corrected). Bars represent standard error of the mean and dots represent individual values.

318

319 *Relationship between tACS phase and perception during visual crowding*

320 Two participants were excluded from the phase analysis due to technical problems that made the
 321 tACS data unavailable. Mean accuracy rates for each phase bin (Supplementary Figure 2), divided
 322 for left and right hemifield, were analysed with a repeated measures ANOVA with two factors
 323 within subjects: Stimulation Condition (10 Hz vs 18 Hz) and Phase Bin (6 levels). Mean accuracy

324 rates for each phase bin when the stimulus was presented in the right hemifield were not affected by
325 the stimulation or tACS phase: indeed, we did not find a significant main effect of the Stimulation
326 Condition ($F_{(1,17)} = 07, p = .79; \eta^2_p = .004$) and Phase Bin ($F_{(5,85)} = .8, p = .55; \eta^2_p = .045$) and the
327 interaction was not significant ($F_{(5,85)} = .21, p = .96; \eta^2_p = .01$). Mean accuracy rates for each phase
328 bin when the stimulus was presented in the left hemifield showed a significant effect of Stimulation
329 Condition ($F_{(1,18)} = 10.2, p = .005; \eta^2_p = .38$) indicating higher performance with 18-Hz tACS, but
330 the factor Phase Bin ($F_{(5,85)} = 1.18, p = .33; \eta^2_p = .07$) and the interaction ($F_{(5,85)} = 1.8, p = .1; \eta^2_p =$
331 $.1$) were not significant (see Supplementary Figure 2).

332 Also the second analysis, which was conducted in order to see whether tACS phase modulated
333 performance according to a sinusoidal function, did not reveal any significant effects (all
334 permutation tests p -values $>.08$; see Supplementary Figure 3).

335

336 *Effects of tACS on EEG activity*

337 Comparing EEG oscillatory power before and after each stimulation session, we observed a
338 significant increment in beta power after 18-Hz tACS ($t_{(19)} = -3.58, p_{\text{corr}} = .008$). On the contrary, no
339 significant differences in beta power were observed after 10-Hz tACS ($t_{(19)} = -0.67, p_{\text{uncorr}} = .255$) and
340 after sham stimulation ($t_{(19)} = -0.30, p_{\text{uncorr}} = .385$) (see Figure 3).

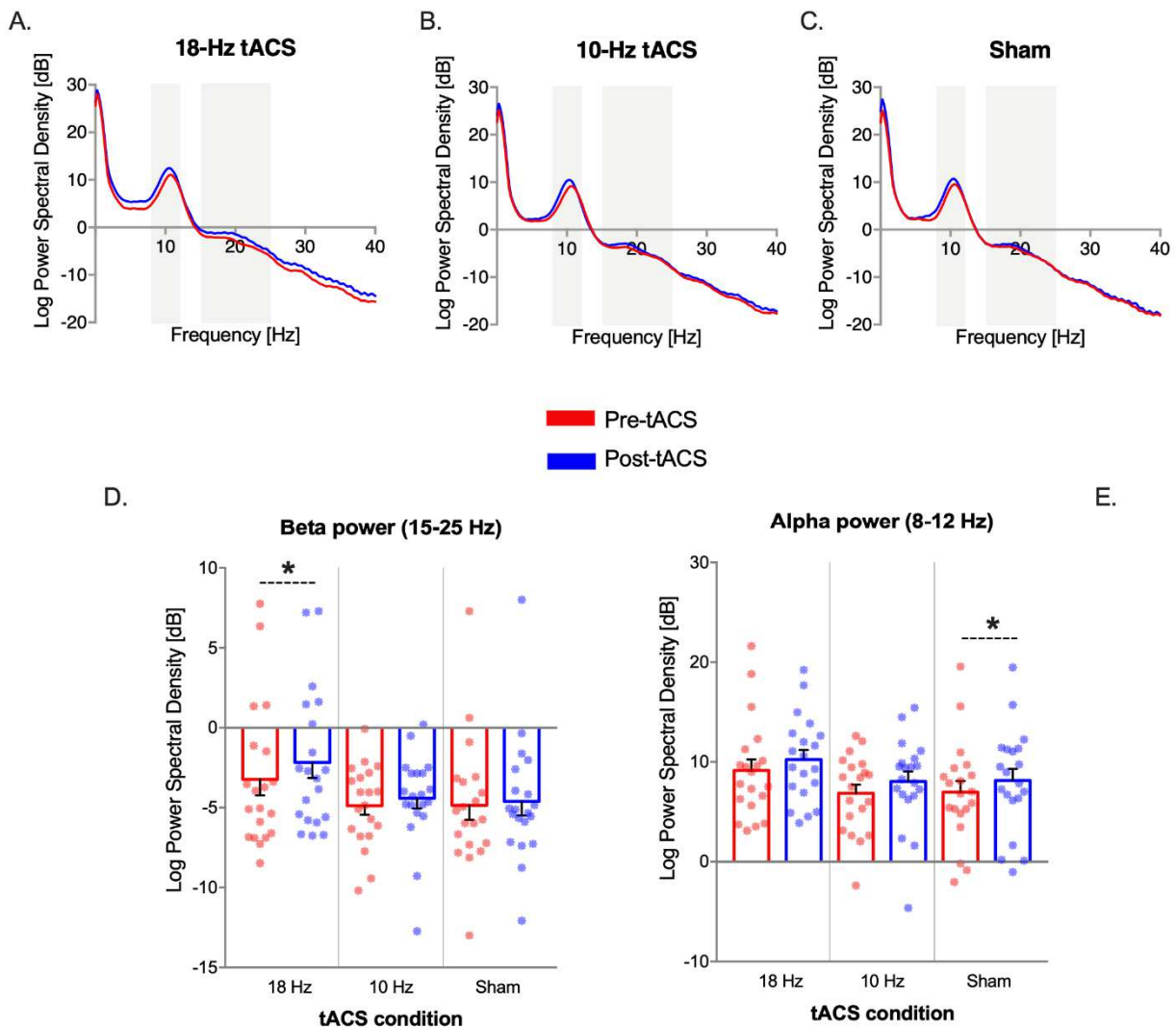
341 When we compared EEG oscillatory variations in the alpha band, we observed a significant
342 increment only after the sham condition ($t_{(19)} = -2.85, p_{\text{corr}} = .041$). On the contrary, no differences in
343 alpha power were observed after 18-Hz tACS ($t_{(19)} = -1.74, p_{\text{corr}} = .39$) and after 10-Hz tACS ($t_{(19)} =$
344 $1.43, p_{\text{uncorr}} = .085$) (see Figure 3).

345 Finally, we performed additional analyses to check whether the power of delta (0.5-4 Hz), theta (4-7
346 Hz) and low-gamma (25-40 Hz) frequency bands changed after 18 Hz tACS. We did not find any
347 significant increment of the power in these other frequency bands (all p s >0.26).

348

349

[Figure 3 about here]



350

351 Figure 3. Effect of tACS on resting-state neural oscillations showing a selective increment of parietal beta (15-25 Hz)
 352 oscillations after 18-Hz tACS. Power spectrum of resting-state EEG before and after 18-Hz (A), 10-Hz (B) or sham (C)
 353 tACS from the channel P4. The frequency band of interest (alpha and beta) are highlighted by the shaded gray areas.
 354 The average power values obtained from these power spectrums are shown in the plots below as a function of the type
 355 of stimulation (i.e. tACS condition) and time of recording (Pre- vs. Post-tACS), separately for the beta (D) and alpha
 356 (E) frequency band. $*=p<.05$ (Bonferroni corrected). Dots represent individual values. Error bars indicate SEM.

357

358 Discussion

359 Visual crowding is a primary bottleneck for conscious object recognition. In this study we
 360 conducted an investigation of possible ways to modulate visual crowding with tACS at different
 361 frequencies. Our aim was to enrich our comprehension of the neural mechanisms of visual

362 crowding. We started from the relationship between visual crowding and beta oscillatory activity
363 (Ronconi et al., 2016; Ronconi and Bellacosa Marotti, 2017) and from the fact that tACS can be a
364 method to shape perceptually relevant brain oscillations (Cecere et al., 2015; Helfrich et al., 2014;
365 Neuling et al., 2012; Stonkus et al., 2016; Wolinski et al., 2018). We hypothesized that tACS within
366 the beta frequency band (18 Hz) would improve the performance in a visual crowding task
367 compared to a control frequency (10 Hz) or to a no stimulation (sham) condition, and tested this
368 hypothesis using a classical crowded letter orientation discrimination paradigm.

369 Our results showed a lower threshold for stimuli presented in the contralateral hemifield and when
370 participants were stimulated with right parietal 18-Hz tACS, as compared to 10-Hz tACS and to the
371 sham stimulation on the same cortical area. The specificity of 18-Hz tACS (vs. 10-Hz tACS) speaks
372 in favour of a precise oscillatory frequency characterizing the activity of the right parietal cortex in
373 crowding tasks. Importantly, the specificity of the effect for the contralateral hemifield was wanted
374 and often used (Battaglini et al., 2017; Bender et al., 2019; Wolinski et al., 2018) to exclude a tACS
375 effect due to participants' differential feeling of sham from real stimulation that would have shown
376 an effect on both visual hemifields.

377 The central aspect of the present findings is a threshold modulation observed for the 18-Hz parietal
378 tACS, whereas stimulation at 10-Hz did not show any effect. This indicates the specificity of the
379 tACS in the beta band applied over the right parietal cortex in resolving crowding. This result is in
380 line with previous EEG studies that showed that beta power, but not alpha, is modulated by the
381 strength of crowding (Ronconi et al., 2016; Ronconi and Bellacosa Marotti, 2017). Moreover, in our
382 study, analysing the resting state EEG activity, we observed that beta parietal tACS was able to
383 induce a significant power increment in the corresponding frequency band, whereas the same effect
384 was not observed with alpha parietal tACS. This evidence is in line with previous findings about the
385 fundamental role of beta oscillations in the excitability of the parietal cortex, as opposed to alpha
386 oscillations that seem to be more related to the occipital cortex excitability (Cabral-Calderin and
387 Wilke, 2019; Samaha et al., 2017).

388 All these results corroborate the link between the beta frequency in the parietal cortex and the visual
389 crowding previously reported in the literature (Ronconi et al., 2016; Ronconi and Bellacosa Marotti,
390 2017). Since in these previous studies visual crowding was found to be related to both event-related
391 beta desynchronization and pre-stimulus beta power, one potential target of the 18-Hz tACS
392 protocol used here could be the interplay between pre-stimulus beta power and event-related beta
393 desynchronization. Indeed, in the literature looking at the behavioural and neurophysiological
394 effects of tACS in the alpha band, there are studies showing that continuous tACS applied during a
395 task is capable of enhancing event-related alpha desynchronization likely by boosting pre-stimulus
396 alpha power (Kasten et al., 2018; Kasten and Herrmann, 2017).

397 One critical aspect of the current finding that needs to be mentioned is that we could not find a
398 significant variation of EEG alpha power over and above the variation observed in the sham
399 condition which has been reported in some previous studies (e.g. Zaehle et al. 2010; Neuling et al.
400 2013; Vossen et al. 2015; Kasten et al. 2016; Kasten and Herrmann 2017). Beyond an intrinsic limit
401 of our experimental design, which did not calculate individual alpha frequency which might have
402 led to different results, we can identify at least three possible reasons for this null effect. First, one
403 major difference that might explain this discrepancy could be that resting EEG has been obtained
404 during eyes-closed condition, and several studies indicate that tACS may not modulate alpha
405 oscillations during eyes-closed states (Neuling et al., 2013; Ruhnau et al., 2016). Second, contrarily
406 to the present study where we used a high-density montage that delivered the electrical current
407 selectively on the right parietal area, some previous studies that found a significant effect of alpha
408 tACS on perception have employed a standard montage with larger stimulation electrodes (e.g.
409 Helfrich et al. 2014; Cecere et al. 2015). Those montages can cause change in activity in many
410 cortical areas at the same time (e.g. occipital and parietal) and thus, it remains to be evaluated
411 whether previously reported behavioural modulation induced by alpha tACS are ultimately due to
412 the stimulation of occipital or parietal areas. Third, we might have targeted a brain region that is not
413 one of the main sources of the alpha activity. At this proposal, recent TMS-EEG evidence support

414 the idea that alpha is the main rhythm of the occipital cortex and beta is the main rhythm of parietal
415 areas. Samaha and colleagues, in particular, found that phosphene perception induced by occipital
416 TMS was influenced by the power of the prestimulus/ongoing EEG in posterior (occipital) regions,
417 while phosphene perception induced by parietal TMS was modulated by the power of EEG beta
418 oscillations (Samaha et al., 2017). Moreover, other TMS studies showed that the dominant EEG
419 oscillatory response evoked by TMS to occipital cortex is within the alpha band, whereas the
420 dominant response after parietal TMS is within the beta band (Rosanova et al. 2009; Ferrarelli et al.
421 2012; for similar findings see Kundu et al. 2014). Overall, these TMS-EEG findings support the
422 existence of partially distinct neural mechanisms that are responsible for alpha and beta activity
423 with influence on perception.

424 Modulation of beta oscillations is often associated to an endogenous perceptual reorganization
425 (Belitski et al., 2008). Indeed, modulation of beta-band power has been associated to the perceptual
426 switch in bi-stable pictures (Ehm et al., 2011; Kornmeier and Bach, 2012; Okazaki et al., 2008),
427 binocular rivalry (Piantoni et al., 2010) and bi-stable motion (Zaretskaya and Bartels, 2015). Beta
428 band power has also been related to other perceptual tasks such as visual form-motion integration
429 (Aissani et al., 2014), perceptual binding of ambiguous visual motion (Costa et al., 2017) and
430 perceptual grouping (Zaretskaya and Bartels, 2015), phenomena that may underlie crowding
431 (Chakravarthi and Pelli, 2011; May and Hess, 2007; Strappini et al., 2017).

432 Consistent with the view that beta oscillations are associated to an endogenous perceptual
433 reorganization, which also occurs when perception switches from crowded to uncrowded, is the
434 hypothesis that the perceptual reorganization promoted by tACS during a crowding task consists in
435 an increase of the efficiency of the mechanism underlying uncrowded perception. But what
436 mechanism would be made more efficient by beta tACS? There is general consent that to perceive
437 an uncrowded visual world the output of detectors activated by several simple features belonging to
438 a target has to be combined into an integrative receptive field of appropriate size for isolating the
439 target from the background (not too large not too small). Fast and automatic feedforward processing

440 in the dorsal stream is inadequate because it only provides information on undetailed basic features
441 (Hochstein and Ahissar, 2002; Jehee et al., 2007) and their spatial location (Vidyasagar and
442 Pammer, 2010). Figure-ground segmentation mechanisms need to be activated in the ventral stream
443 or in lower level areas in order to select the appropriate (smaller) receptive fields (Lamme and
444 Roelfsema, 2000; Lee et al., 1998) for isolating the target from flankers. There is general consent
445 that interactions between higher and lower visual areas through activation of feedback would be
446 needed in order to activate these visual filters with small, high-resolution receptive field and obtain
447 a detailed representation of visual images (Hochstein and Ahissar, 2002; Jehee et al., 2007; Lamme
448 and Roelfsema, 2000; Lee et al., 1998).

449 We speculate that, by synchronizing the activity of parietal areas with the tACS at the appropriate
450 frequency, it is possible to promote long-range synchrony between bottom-up and top-down
451 processing involved in visual perception (Costa et al., 2017) and the dorso-ventral feedback might
452 become more efficient and facilitate local information processing, thus inducing a good
453 discrimination of target from flankers and inducing active disambiguation. Some studies might
454 support our speculation. For example, it has been shown that beta band connectivity is the
455 preferential rhythm for communication within the right fronto-parietal network (that gives top-down
456 feedback to ventral areas for selecting spatial location for further processing) during spatial
457 attention tasks (Siegel et al., 2008). Patterns of rhythmic beta TMS stimulation in frontal right areas
458 lead to greater entrainment of local oscillations and to higher conscious detection of contralateral
459 stimulus compared to random patterns (Vernet et al., 2019) and visual alertness processes correlate
460 with a prestimulus beta band activation (Britz et al., 2011). Interestingly, 18-Hz tACS facilitation
461 was found especially when the target-flanker distance was at threshold level, suggesting that dorso-
462 ventral feedback becomes more effective in local information processing when the stimulus
463 configuration is ambiguous (in our task, close H flankers can make ambiguous the orientation of the
464 T target).

465 Given that the effects of 18-Hz tACS was found with tACS applied to parietal cortex, we suggest
466 that the parietal cortex activation contributes to the changes from global (crowded) to local
467 (uncrowded) perception mediated by dorso-ventral feedback. These perceptual changes are not
468 exogenously driven but rather endogenously driven by the task, and possibly mediated by feature-
469 based attention (Vidyasagar and Pammer, 2010). This suggestion is consistent with previous studies
470 showing that switches in perception have been related to the parietal cortex activation (Britz et al.,
471 2011, 2009; Carmel et al., 2010; Kanai et al., 2010). Our results therefore confirm the suggestion
472 that the parietal beta-band activity plays a role in internally, rather than externally driven changes in
473 perceptual processing (Zaretskaya and Bartels, 2015).

474 Resting state EEG activity showed that only beta parietal stimulation was able to induce a
475 significant power increment in the corresponding frequency band in line with previous studies that
476 showed that beta activity is predictive of the excitability of the parietal cortex (Cabral-Calderin and
477 Wilke, 2019; Samaha et al., 2017). On the contrary, we did not observe a comparable significant
478 alpha power increment after the 10-Hz tACS, but we observed only an alpha power enhancement
479 after sham, which might be caused by tiredness after the task (Benwell et al., 2019).

480 We also tested whether there was an association between specific 18-Hz tACS phase and
481 performance when the stimulus was presented in the left hemifield, or if the modulation of
482 performance followed a sinusoidal function as it would be predicted by a true neural entrainment
483 effect. In both analyses, we did not find a significant modulation of task accuracy as a function of
484 tACS phase. There is a growing number of studies showing the importance of tACS phase at the
485 onset of the stimulus. Polanía and colleagues (Polanía et al., 2012) showed a decrease of reaction
486 time during a working memory task during a specific phase of 6Hz theta tACS delivered over the
487 frontal and parietal areas. Helfrich and colleagues (Helfrich et al., 2014) using a visual oddball
488 paradigm showed that the phase of the tACS modulates target detection performance. Similarly,
489 Neuling et al. (Neuling et al., 2012) showed that the perception of auditory stimuli embedded in
490 noise was modulated by the phase of tACS delivered within the alpha frequency. Most of the

491 studies targeting theta/alpha oscillations with tACS suggest that a stimulus can be elaborated better
492 during a specific phase of the alpha wave that is associated to higher neural excitability. However,
493 at present there is no neurophysiological evidence of a clear relationship between the phase of beta
494 oscillations and neural excitability. Thus, applying the same logic of ‘duty cycle’ (i.e. the one half
495 of the alpha cycle associated to a better perception and higher neural activity) to beta oscillations
496 may be misleading (Samaha et al., 2017). The majority of previous studies looking at the
497 relationship between theta/alpha tACS phase and perception/cognition interpreted the observed
498 effects as the consequence of the entrainment of endogenous neural oscillations, based on
499 behavioural (Neuling et al., 2012), EEG (Stonkus et al., 2016) or both (Helfrich et al., 2014)
500 evidence. In the present study, on the one hand we found a significant modulation of EEG beta band
501 power after tACS, which is one of the criteria to establish the presence of neural entrainment;
502 indeed, an increased post-tACS EEG power is supposed to reflect a large population of neurons that
503 become phase aligned to the tACS frequency and resonate at this frequency even after the end of
504 the stimulation (Hanslmayr et al., 2019; Romei et al., 2011). Another evidence would be the
505 presence of phase alignment of the population activity to the entraining tACS frequency during the
506 stimulation itself (Hanslmayr et al., 2019). In our study however, we cannot test this second
507 criterion because we did not record EEG data during the stimulation. It is important to note,
508 however, that these data would be massively contaminated by tACS artefacts and, at present, there
509 is no agreement in the literature on what is the best approach to remove them (e.g. see Noury et al.,
510 2016; Noury and Siegel, 2017). A third sign of entrainment of brain oscillation would be a
511 significant modulation of task accuracy by tACS phase, especially if such modulation follows a
512 sinusoidal function. In our data, however, we did not find evidence of a phasic modulation of
513 accuracy. This could be possibly attributable to the limited number of trials going into each phase
514 bin (for a recent discussion of different phase analysis approaches see Zoefel et al., 2019), and
515 future studies are needed to better address this question with appropriate statistical power.

516 In conclusion, we found that 18 Hz electrical stimulation of the parietal cortex enhanced perceptual
517 discrimination in conditions of visual crowding. Our results showed a hemifield-specific effect and
518 a frequency-specific effect, which constitute two important internal controls for this study.
519 The demonstration that parietal tACS at beta frequency not only impacts on behaviour but also
520 significantly affects endogenous oscillatory dynamics suggest, more broadly, that the efficiency of
521 the right dorsal fronto-parietal network can be modulated by tACS at relevant frequencies, with
522 potential applications in many other aspects of perception and cognition, such as reading (Barollo et
523 al., 2017; Bertoni et al., 2019; Zorzi et al., 2012). Our findings constitute the first demonstration
524 that visual crowding can be reduced through the application of beta neurostimulation in the parietal
525 area and contributes to enlighten the neural mechanisms and the oscillatory fingerprint of a
526 fundamental aspect of human vision.

527

528

529

530

531 **Disclosure of funding sources:** The study was supported by a grant from MIUR (Dipartimenti di
532 Eccellenza DM 11/05/2017 n.262) to the Department of General Psychology

533 **Disclosure of potential conflict of interest:** The authors declare no competing interests.

534

535 **Reference**

- 536 Aissani, C., Martinerie, J., Yahia-Cherif, L., Paradis, A.-L., Lorenceau, J., 2014. Beta, but Not Gamma, Band
537 Oscillations Index Visual Form-Motion Integration. *PLoS One* 9, e95541.
538 <https://doi.org/10.1371/journal.pone.0095541>
- 539 Antal, A., Alekseichuk, I., Bikson, M., Brockmüller, J., Brunoni, A.R., Chen, R., Cohen, L.G., Douthwaite,
540 G., Ellrich, J., Flöel, A., Fregni, F., George, M.S., Hamilton, R., Haueisen, J., Herrmann, C.S.,
541 Hummel, F.C., Lefaucheur, J.P., Liebetanz, D., Loo, C.K., McCaig, C.D., Miniussi, C., Miranda, P.C.,
542 Moliadze, V., Nitsche, M.A., Nowak, R., Padberg, F., Pascual-Leone, A., Poppendieck, W., Priori, A.,
543 Rossi, S., Rossini, P.M., Rothwell, J., Rueger, M.A., Ruffini, G., Schellhorn, K., Siebner, H.R., Ugawa,
544 Y., Wexler, A., Ziemann, U., Hallett, M., Paulus, W., 2017. Low intensity transcranial electric
545 stimulation: Safety, ethical, legal regulatory and application guidelines. *Clin. Neurophysiol.* 128, 1774–
546 1809. <https://doi.org/10.1016/J.CLINPH.2017.06.001>
- 547 Barollo, M., Contemori, G., Battaglini, L., Pavan, A., Casco, C., 2017. Perceptual learning improves contrast
548 sensitivity, visual acuity, and foveal crowding in amblyopia. *Restor. Neurol. Neurosci.* 35.
549 <https://doi.org/10.3233/RNN-170731>
- 550 Battaglini, L., Noventa, S., Casco, C., 2017. Anodal and cathodal electrical stimulation over V5 improves
551 motion perception by signal enhancement and noise reduction. *Brain Stimul.* 10.
552 <https://doi.org/10.1016/j.brs.2017.04.128>
- 553 Belitski, A., Gretton, A., Magri, C., Murayama, Y., Montemurro, M.A., Logothetis, N.K., Panzeri, S., 2008.
554 Low-Frequency Local Field Potentials and Spikes in Primary Visual Cortex Convey Independent
555 Visual Information. *J. Neurosci.* 28, 5696–5709. <https://doi.org/10.1523/JNEUROSCI.0009-08.2008>
- 556 Bender, M., Romei, V., Sauseng, P., 2019. Slow Theta tACS of the Right Parietal Cortex Enhances
557 Contralateral Visual Working Memory Capacity. *Brain Topogr.* 32, 477–481.
558 <https://doi.org/10.1007/s10548-019-00702-2>
- 559 Benwell, C.S.Y., London, R.E., Tagliabue, C.F., Veniero, D., Gross, J., Keitel, C., Thut, G., 2019. Frequency
560 and power of human alpha oscillations drift systematically with time-on-task. *Neuroimage* 192, 101–
561 114. <https://doi.org/10.1016/J.NEUROIMAGE.2019.02.067>
- 562 Bertoni, S., Franceschini, S., Ronconi, L., Gori, S., Facoetti, A., 2019. Is excessive visual crowding causally

- 563 linked to developmental dyslexia? *Neuropsychologia*.
- 564 <https://doi.org/10.1016/J.NEUROPSYCHOLOGIA.2019.04.018>
- 565 Bonnef, Y.S., Sagi, D., Polat, U., 2007. Spatial and temporal crowding in amblyopia. *Vision Res.* 47, 1950–
- 566 1962. <https://doi.org/10.1016/J.VISRES.2007.02.015>
- 567 Brainard, D.H., 1997. The Psychophysics Toolbox. *Spat. Vis.* 10, 433–436.
- 568 <https://doi.org/10.1163/156856897X00357>
- 569 Britz, J., Landis, T., Michel, C.M., 2009. Right Parietal Brain Activity Precedes Perceptual Alternation of
- 570 Bistable Stimuli. *Cereb. Cortex* 19, 55–65. <https://doi.org/10.1093/cercor/bhn056>
- 571 Britz, J., Pitts, M.A., Michel, C.M., 2011. Right parietal brain activity precedes perceptual alternation during
- 572 binocular rivalry. *Hum. Brain Mapp.* 32, 1432–1442. <https://doi.org/10.1002/hbm.21117>
- 573 Cabral-Calderin, Y., Wilke, M., 2019. Probing the Link Between Perception and Oscillations: Lessons from
- 574 Transcranial Alternating Current Stimulation. *Neuroscientist*.
- 575 <https://doi.org/10.1177/1073858419828646>
- 576 Carmel, D., Walsh, V., Lavie, N., Rees, G., 2010. Right parietal TMS shortens dominance durations in
- 577 binocular rivalry. *Curr. Biol.* 20, R799–R800. <https://doi.org/10.1016/J.CUB.2010.07.036>
- 578 Cecere, R., Rees, G., Romei, V., 2015. Individual Differences in Alpha Frequency Drive Crossmodal
- 579 Illusory Perception. *Curr. Biol.* 25, 231–235. <https://doi.org/10.1016/j.cub.2014.11.034>
- 580 Chakravarthi, R., Pelli, D.G., 2011. The same binding in contour integration and crowding. *J. Vis.* 11, 10–10.
- 581 <https://doi.org/10.1167/11.8.10>
- 582 Chen, J., He, Y., Zhu, Z., Zhou, T., Peng, Y., Zhang, X., Fang, F., 2014. Attention-Dependent Early Cortical
- 583 Suppression Contributes to Crowding. *J. Neurosci.* 34, 10465–10474.
- 584 <https://doi.org/10.1523/jneurosci.1140-14.2014>
- 585 Chicherov, V., Plomp, G., Herzog, M.H., 2014. Neural correlates of visual crowding. *Neuroimage* 93, 23–
- 586 31. <https://doi.org/10.1016/J.NEUROIMAGE.2014.02.021>
- 587 Costa, G.N., Duarte, J.V., Martins, R., Wibral, M., Castelo-Branco, M., 2017. Interhemispheric Binding of
- 588 Ambiguous Visual Motion Is Associated with Changes in Beta Oscillatory Activity but Not with
- 589 Gamma Range Synchrony. *J. Cogn. Neurosci.* 29, 1829–1844. https://doi.org/10.1162/jocn_a_01158
- 590 Delorme, A., Makeig, S., 2004. EEGLAB: an open source toolbox for analysis of single-trial EEG dynamics

- 591 including independent component analysis. *J. Neurosci. Methods* 134, 9–21.
592 <https://doi.org/10.1016/J.JNEUMETH.2003.10.009>
- 593 Di Russo, F., Martínez, A., Sereno, M.I., Pitzalis, S., Hillyard, S.A., 2002. Cortical sources of the early
594 components of the visual evoked potential. *Hum. Brain Mapp.* 15, 95–111.
595 <https://doi.org/10.1002/hbm.10010>
- 596 Ehm, W., Bach, M., Kornmeier, J., 2011. Ambiguous figures and binding: EEG frequency modulations
597 during multistable perception. *Psychophysiology* 48, 547–558. [https://doi.org/10.1111/j.1469-](https://doi.org/10.1111/j.1469-8986.2010.01087.x)
598 [8986.2010.01087.x](https://doi.org/10.1111/j.1469-8986.2010.01087.x)
- 599 Ferrarelli, F., Sarasso, S., Guller, Y., Riedner, B.A., Peterson, M.J., Bellesi, M., Massimini, M., Postle, B.R.,
600 Tononi, G., 2012. Reduced Natural Oscillatory Frequency of Frontal Thalamocortical Circuits in
601 Schizophrenia. *Arch. Gen. Psychiatry* 69, 766–774.
602 <https://doi.org/10.1001/archgenpsychiatry.2012.147>
- 603 Fertonani, A., Ferrari, C., Miniussi, C., 2015. What do you feel if I apply transcranial electric stimulation?
604 Safety, sensations and secondary induced effects. *Clin. Neurophysiol.* 126, 2181–2188.
605 <https://doi.org/10.1016/J.CLINPH.2015.03.015>
- 606 Freeman, J., Simoncelli, E., 2010. Crowding and metamerism in the ventral stream. *J. Vis.* 10, 1347–1347.
607 <https://doi.org/10.1167/10.7.1347>
- 608 Fröhlich, F., McCormick, D.A., 2010. Endogenous electric fields may guide neocortical network activity.
609 *Neuron* 67, 129–143. <https://doi.org/10.1016/j.neuron.2010.06.005>
- 610 Gori, S., Facoetti, A., 2015. How the visual aspects can be crucial in reading acquisition? The intriguing case
611 of crowding and developmental dyslexia. *J. Vis.* 15, 8–8. <https://doi.org/10.1167/15.1.8>
- 612 Green, C.S., Bavelier, D., 2007. Action-Video-Game Experience Alters the Spatial Resolution of Vision.
613 *Psychol. Sci.* 18, 88–94. <https://doi.org/10.1111/j.1467-9280.2007.01853.x>
- 614 Han, Q., Luo, H., 2019. Visual crowding involves delayed frontoparietal response and enhanced top-down
615 modulation. *Eur. J. Neurosci.* 1–11. <https://doi.org/10.1111/ejn.14401>
- 616 Hanslmayr, S., Axmacher, N., Inman, C.S., 2019. Modulating Human Memory via Entrainment of Brain
617 Oscillations. *Trends Neurosci.* <https://doi.org/10.1016/j.tins.2019.04.004>
- 618 Helfrich, R.F., Schneider, T.R., Rach, S., Trautmann-Lengsfeld, S.A., Engel, A.K., Herrmann, C.S., 2014.

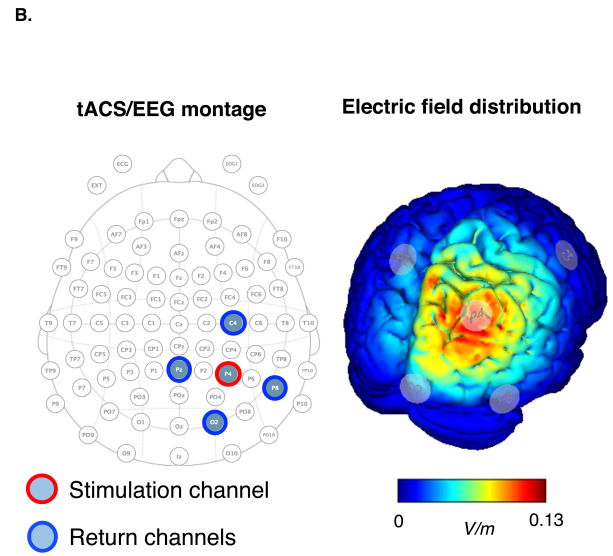
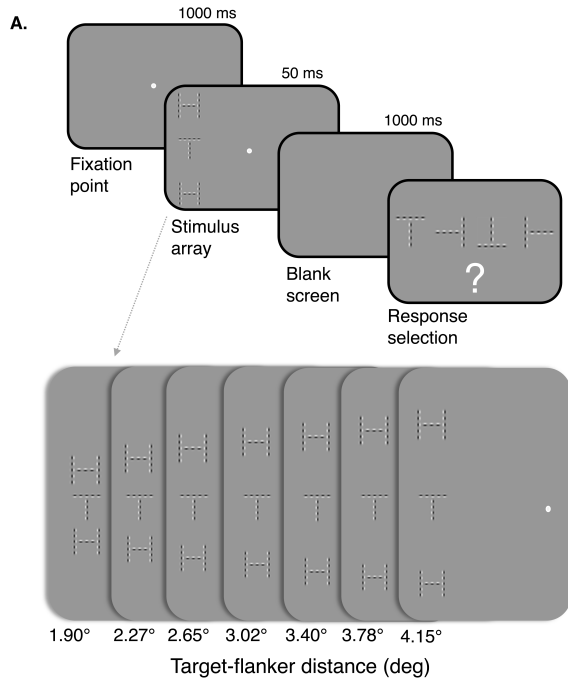
- 619 Entrainment of brain oscillations by transcranial alternating current stimulation. *Curr. Biol.* 24, 333–
620 339. <https://doi.org/10.1016/j.cub.2013.12.041>
- 621 Herrmann, C.S., Strüber, D., Helfrich, R.F., Engel, A.K., 2016. EEG oscillations: From correlation to
622 causality. *Int. J. Psychophysiol.* <https://doi.org/10.1016/j.ijpsycho.2015.02.003>
- 623 Herzog, M.H., Manassi, M., 2015. Uncorking the bottleneck of crowding: A fresh look at object recognition.
624 *Curr. Opin. Behav. Sci.* 1, 86–93. <https://doi.org/10.1016/j.cobeha.2014.10.006>
- 625 Hochstein, S., Ahissar, M., 2002. View from the Top: Hierarchies and Reverse Hierarchies in the Visual
626 System. *Neuron* 36, 791–804. [https://doi.org/10.1016/S0896-6273\(02\)01091-7](https://doi.org/10.1016/S0896-6273(02)01091-7)
- 627 Jehee, J.F.M., Roelfsema, P.R., Deco, G., Murre, J.M.J., Lamme, V.A.F., 2007. Interactions between higher
628 and lower visual areas improve shape selectivity of higher level neurons-Explaining crowding
629 phenomena. *Brain Res.* 1157, 167–176. <https://doi.org/10.1016/j.brainres.2007.03.090>
- 630 Kanai, R., Bahrami, B., Rees, G., 2010. Human Parietal Cortex Structure Predicts Individual Differences in
631 Perceptual Rivalry. *Curr. Biol.* 20, 1626–1630. <https://doi.org/10.1016/J.CUB.2010.07.027>
- 632 Kasten, F.H., Dowsett, J., Herrmann, C.S., 2016. Sustained Aftereffect of α -tACS Lasts Up to 70 min after
633 Stimulation. *Front. Hum. Neurosci.* 10, 245. <https://doi.org/10.3389/fnhum.2016.00245>
- 634 Kasten, F.H., Herrmann, C.S., 2017. Transcranial Alternating Current Stimulation (tACS) Enhances Mental
635 Rotation Performance during and after Stimulation. *Front. Hum. Neurosci.* 11, 2.
636 <https://doi.org/10.3389/fnhum.2017.00002>
- 637 Kasten, F.H., Maess, B., Herrmann, C.S., 2018. Facilitated event-related power modulations during
638 transcranial alternating current stimulation (tACS) revealed by concurrent tACSMEG. *eNeuro* 5.
639 <https://doi.org/10.1523/ENEURO.0069-18.2018>
- 640 Kingdom, F.A.A., Prins, N., 2016. *Psychophysics : a practical introduction*. Elsevier Academic Press.
- 641 Kornmeier, J., Bach, M., 2012. Ambiguous Figures – What Happens in the Brain When Perception Changes
642 But Not the Stimulus. *Front. Hum. Neurosci.* 6, 51. <https://doi.org/10.3389/fnhum.2012.00051>
- 643 Kundu, B., Johnson, J.S., Postle, B.R., 2014. Prestimulation phase predicts the TMS-evoked response. *J.*
644 *Neurophysiol.* 112, 1885–1893. <https://doi.org/10.1152/jn.00390.2013>
- 645 Laczó, B., Antal, A., Niebergall, R., Treue, S., Paulus, W., 2012. Transcranial alternating stimulation in a
646 high gamma frequency range applied over V1 improves contrast perception but does not modulate

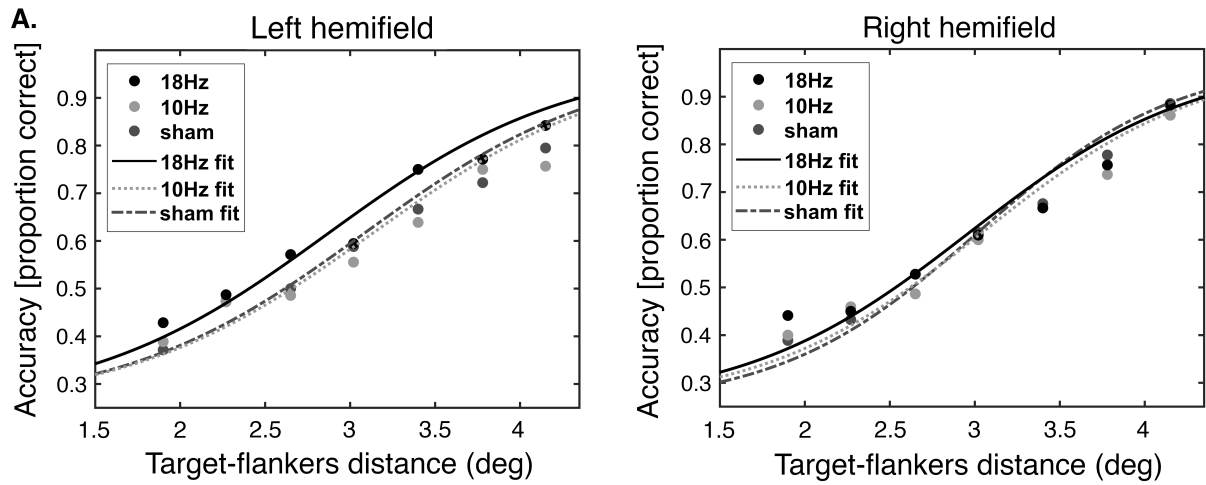
- 647 spatial attention. *Brain Stimul.* 5, 484–491. <https://doi.org/10.1016/J.BRS.2011.08.008>
- 648 Lamme, V.A.F., Roelfsema, P.R., 2000. The distinct modes of vision offered by feedforward and recurrent
649 processing. *Trends Neurosci.* 23, 571–579. [https://doi.org/10.1016/S0166-2236\(00\)01657-X](https://doi.org/10.1016/S0166-2236(00)01657-X)
- 650 Lee, T.S., Mumford, D., Romero, R., Lamme, V.A.F., 1998. The role of the primary visual cortex in higher
651 level vision. *Vision Res.* 38, 2429–2454. [https://doi.org/10.1016/S0042-6989\(97\)00464-1](https://doi.org/10.1016/S0042-6989(97)00464-1)
- 652 Levi, D.M., 2008. Crowding—An essential bottleneck for object recognition: A mini-review. *Vision Res.* 48,
653 635–654. <https://doi.org/10.1016/J.VISRES.2007.12.009>
- 654 Levy, T., Walsh, V., Lavidor, M., 2010. Dorsal stream modulation of visual word recognition in skilled
655 readers. *Vision Res.* 50, 883–888. <https://doi.org/10.1016/J.VISRES.2010.02.019>
- 656 May, K.A., Hess, R.F., 2007. Ladder contours are undetectable in the periphery: A crowding effect? *J. Vis.*
657 7, 9. <https://doi.org/10.1167/7.13.9>
- 658 Moll, K., Jones, M., 2013. Naming fluency in dyslexic and nondyslexic readers: Differential effects of visual
659 crowding in foveal, parafoveal, and peripheral vision. *Q. J. Exp. Psychol.* 66, 2085–2091.
660 <https://doi.org/10.1080/17470218.2013.840852>
- 661 Neuling, T., Rach, S., Herrmann, C.S., 2013. Orchestrating neuronal networks: sustained after-effects of
662 transcranial alternating current stimulation depend upon brain states. *Front. Hum. Neurosci.* 7, 161.
663 <https://doi.org/10.3389/fnhum.2013.00161>
- 664 Neuling, T., Rach, S., Wagner, S., Wolters, C.H., Herrmann, C.S., 2012. Good vibrations: Oscillatory phase
665 shapes perception. *Neuroimage* 63, 771–778. <https://doi.org/10.1016/j.neuroimage.2012.07.024>
- 666 Noury, N., Hipp, J.F., Siegel, M., 2016. Physiological processes non-linearly affect electrophysiological
667 recordings during transcranial electric stimulation. *Neuroimage* 140, 99–109.
668 <https://doi.org/10.1016/j.neuroimage.2016.03.065>
- 669 Noury, N., Siegel, M., 2017. Phase properties of transcranial electrical stimulation artifacts in
670 electrophysiological recordings. *Neuroimage* 158, 406–416.
671 <https://doi.org/10.1016/j.neuroimage.2017.07.010>
- 672 Okazaki, M., Kaneko, Y., Yumoto, M., Arima, K., 2008. Perceptual change in response to a bistable picture
673 increases neuromagnetic beta-band activities. *Neurosci. Res.* 61, 319–328.
674 <https://doi.org/10.1016/j.neures.2008.03.010>

- 675 Omtzigt, D., Hendriks, A.W., Kolk, H.H., 2002. Evidence for magnocellular involvement in the
676 identification of flanked letters. *Neuropsychologia* 40, 1881–1890. [https://doi.org/10.1016/S0028-](https://doi.org/10.1016/S0028-3932(02)00069-6)
677 [3932\(02\)00069-6](https://doi.org/10.1016/S0028-3932(02)00069-6)
- 678 Pelli, D.G., 2008. Crowding: a cortical constraint on object recognition. *Curr. Opin. Neurobiol.* 18, 445–451.
679 <https://doi.org/10.1016/J.CONB.2008.09.008>
- 680 Pelli, D.G., 1997. The VideoToolbox software for visual psychophysics: Transforming numbers into movies.
681 *Spat. Vis.* 10, 437–442. <https://doi.org/10.1163/156856897X00366>
- 682 Peng, C., Hu, C., Chen, Y., 2018. The temporal dynamic relationship between attention and crowding:
683 Electrophysiological evidence from an event-related potential study. *Front. Neurosci.* 12, 1–11.
684 <https://doi.org/10.3389/fnins.2018.00844>
- 685 Piantoni, G., Kline, K.A., Eagleman, D.M., 2010. Beta oscillations correlate with the probability of
686 perceiving rivalrous visual stimuli. *J. Vis.* 10, 18–18. <https://doi.org/10.1167/10.13.18>
- 687 Polanía, R., Nitsche, M.A., Korman, C., Batsikadze, G., Paulus, W., 2012. The Importance of Timing in
688 Segregated Theta Phase-Coupling for Cognitive Performance. *Curr. Biol.* 22, 1314–1318.
689 <https://doi.org/10.1016/J.CUB.2012.05.021>
- 690 Prins, N., Kingdom, F.A.A., 2018. Applying the Model-Comparison Approach to Test Specific Research
691 Hypotheses in Psychophysical Research Using the Palamedes Toolbox. *Front. Psychol.* 9, 1250.
692 <https://doi.org/10.3389/FPSYG.2018.01250>
- 693 Robol, V., Grassi, M., Casco, C., 2013. Contextual influences in texture-segmentation: Distinct effects from
694 elements along the edge and in the texture-region. *Vision Res.* 88, 1–8.
695 <https://doi.org/10.1016/J.VISRES.2013.05.010>
- 696 Romei, V., Driver, J., Schyns, P.G., Thut, G., 2011. Rhythmic TMS over Parietal Cortex Links Distinct
697 Brain Frequencies to Global versus Local Visual Processing. *Curr. Biol.* 21, 334–337.
698 <https://doi.org/10.1016/J.CUB.2011.01.035>
- 699 Romei, V., Thut, G., Mok, R.M., Schyns, P.G., Driver, J., 2012. Causal implication by rhythmic transcranial
700 magnetic stimulation of alpha frequency in feature-based local vs. global attention. *Eur. J. Neurosci.* 35,
701 968–974. <https://doi.org/10.1111/j.1460-9568.2012.08020.x>
- 702 Ronconi, L., Bellacosa Marotti, R., 2017. Awareness in the crowd: Beta power and alpha phase of

- 703 prestimulus oscillations predict object discrimination in visual crowding. *Conscious. Cogn.* 54, 36–46.
704 <https://doi.org/10.1016/j.concog.2017.04.020>
- 705 Ronconi, L., Bertoni, S., Bellacosa Marotti, R., 2016. The neural origins of visual crowding as revealed by
706 event-related potentials and oscillatory dynamics. *Cortex* 79, 87–98.
707 <https://doi.org/10.1016/J.CORTEX.2016.03.005>
- 708 Rosanova, M., Casali, A., Bellina, V., Resta, F., Mariotti, M., Massimini, M., 2009. Natural frequencies of
709 human corticothalamic circuits. *J. Neurosci.* 29, 7679–85. [https://doi.org/10.1523/JNEUROSCI.0445-](https://doi.org/10.1523/JNEUROSCI.0445-09.2009)
710 [09.2009](https://doi.org/10.1523/JNEUROSCI.0445-09.2009)
- 711 Ruhnau, P., Neuling, T., Fuscá, M., Herrmann, C.S., Demarchi, G., Weisz, N., 2016. Eyes wide shut:
712 Transcranial alternating current stimulation drives alpha rhythm in a state dependent manner. *Sci. Rep.*
713 6, 27138. <https://doi.org/10.1038/srep27138>
- 714 Samaha, J., Gosseries, O., Postle, B.R., 2017. Distinct Oscillatory Frequencies Underlie Excitability of
715 Human Occipital and Parietal Cortex. *J. Neurosci.* 37, 2824–2833.
716 <https://doi.org/10.1523/JNEUROSCI.3413-16.2017>
- 717 Siegel, M., Donner, T.H., Oostenveld, R., Fries, P., Engel, A.K., 2008. Neuronal Synchronization along the
718 Dorsal Visual Pathway Reflects the Focus of Spatial Attention. *Neuron* 60, 709–719.
719 <https://doi.org/10.1016/J.NEURON.2008.09.010>
- 720 Stonkus, R., Braun, V., Kerlin, J.R., Volberg, G., Hanslmayr, S., 2016. Probing the causal role of prestimulus
721 interregional synchrony for perceptual integration via tACS. *Sci. Rep.* 6, 32065.
722 <https://doi.org/10.1038/srep32065>
- 723 Strappini, F., Galati, G., Martelli, M., Di Pace, E., Pitzalis, S., 2017. Perceptual integration and attention in
724 human extrastriate cortex. *Sci. Rep.* 7. <https://doi.org/10.1038/s41598-017-13921-z>
- 725 Strüber, D., Rach, S., Trautmann-Lengsfeld, S.A., Engel, A.K., Herrmann, C.S., 2014. Antiphase 40 Hz
726 Oscillatory Current Stimulation Affects Bistable Motion Perception. *Brain Topogr.* 27, 158–171.
727 <https://doi.org/10.1007/s10548-013-0294-x>
- 728 Vernet, M., Stengel, C., Quentin, R., Amengual, J.L., Valero-Cabré, A., 2019. Entrainment of local
729 synchrony reveals a causal role for high-beta right frontal oscillations in human visual consciousness.
730 *bioRxiv* 574939. <https://doi.org/10.1101/574939>

- 731 Vidyasagar, T.R., 2004. Neural underpinnings of dyslexia as a disorder of visuo-spatial attention. *Clin. Exp.*
732 *Optom.* 87, 4–10. <https://doi.org/10.1111/j.1444-0938.2004.tb03138.x>
- 733 Vidyasagar, T.R., 1999. A neuronal model of attentional spotlight: parietal guiding the temporal. *Brain Res.*
734 *Rev.* 30, 66–76. [https://doi.org/10.1016/S0165-0173\(99\)00005-3](https://doi.org/10.1016/S0165-0173(99)00005-3)
- 735 Vidyasagar, T.R., Pammer, K., 2010. Dyslexia: a deficit in visuo-spatial attention, not in phonological
736 processing. *Trends Cogn. Sci.* 14, 57–63. <https://doi.org/10.1016/J.TICS.2009.12.003>
- 737 Vossen, A., Gross, J., Thut, G., 2015. Alpha Power Increase After Transcranial Alternating Current
738 Stimulation at Alpha Frequency (α -tACS) Reflects Plastic Changes Rather Than Entrainment. *Brain*
739 *Stimul.* 8, 499–508. <https://doi.org/10.1016/J.BRS.2014.12.004>
- 740 Whitney, D., Levi, D.M., 2011. Visual crowding: A fundamental limit on conscious perception and object
741 recognition. *Trends Cogn. Sci.* <https://doi.org/10.1016/j.tics.2011.02.005>
- 742 Wolinski, N., Cooper, N.R., Sauseng, P., Romei, V., 2018. The speed of parietal theta frequency drives
743 visuospatial working memory capacity. *PLoS Biol.* 16. <https://doi.org/10.1371/journal.pbio.2005348>
- 744 Zaehle, T., Rach, S., Herrmann, C.S., 2010. Transcranial Alternating Current Stimulation Enhances
745 Individual Alpha Activity in Human EEG. *PLoS One* 5, e13766.
746 <https://doi.org/10.1371/journal.pone.0013766>
- 747 Zaretskaya, N., Bartels, A., 2015. Gestalt perception is associated with reduced parietal beta oscillations.
748 *Neuroimage* 112, 61–69. <https://doi.org/10.1016/J.NEUROIMAGE.2015.02.049>
- 749 Zoefel, B., Davis, M.H., Valente, G., Riecke, L., 2019. How to test for phasic modulation of neural and
750 behavioural responses. *Neuroimage* 202, 116175. <https://doi.org/10.1016/j.neuroimage.2019.116175>
- 751 Zorzi, M., Barbiero, C., Facoetti, A., Lonciari, I., Carrozzi, M., Montico, M., Bravar, L., George, F., Pech-
752 Georgel, C., Ziegler, J.C., 2012. Extra-large letter spacing improves reading in dyslexia. *Proc. Natl.*
753 *Acad. Sci.* 109, 11455–11459. <https://doi.org/10.1073/pnas.1205566109>
- 754





B. Crowding threshold

